GEOLOGY | THE GEOLOGICAL SOCIETY OF AMERICA®

https://doi.org/10.1130/G52432.1

Manuscript received 30 May 2024
Revised manuscript received 8 October 2024
Manuscript accepted 23 October 2024

Published online 8 November 2024

North Pacific warmth synchronous with the Miocene Climatic Optimum

Jared E. Nirenberg* and Timothy D. Herbert
Department of Earth, Environmental, and Planetary Sciences, Brown University, Providence, Rhode Island 02912, USA

ABSTRACT

Peak Neogene warmth and minimal polar ice volumes occurred during the Miocene Climatic Optimum (MCO, ca. 16.95–13.95 Ma) followed by cooling and ice sheet expansion during the Middle Miocene Climate Transition (MMCT, ca. 13.95–12.8 Ma). Previous records of northern high-latitude sea surface temperatures (SSTs) during these global climatic transitions are limited to Atlantic sites, and none resolve orbital-scale variability. Here, we present an orbital-resolution alkenone SST proxy record from the subpolar North Pacific that establishes a local maximum of SSTs during the MCO as much as 16 °C warmer than modern with rapid warming initiating the MCO, cooling synchronous with Antarctic ice sheet expansion during the MMCT, and high variability on orbital time scales. Persistently cooler North Pacific SST anomalies than in the Atlantic at equivalent latitudes throughout the Miocene suggest enhanced Atlantic northward heat transport under a globally warm climate. We conclude that a global forcing mechanism, likely elevated greenhouse gas concentrations, is the most parsimonious explanation for synchronous global high-latitude warmth during the Miocene.

INTRODUCTION

The middle Miocene is distinguished as the major warm anomaly in the Cenozoic transition from global greenhouse conditions to the modern icehouse world (Westerhold et al., 2020). During the Miocene Climatic Optimum (MCO, ca. 16.95–13.95 Ma), ice sheets retreated, leaving Antarctica at least partially deglaciated and occupied with temperate and tundra ecosystems (Lewis et al., 2008; Warny et al., 2009). Cooling and ice sheet growth intensified during the Middle Miocene Climate Transition (MMCT, ca. 13.95–12.8 Ma), culminating in the reestablishment and expansion of the East Antarctic Ice Sheet during the Mi3 glaciation (ca. 13.8–13.9 Ma; Miller et al., 1991). Outside of Antarctica, global ecosystems shifted from equable MCO conditions toward stronger meridional gradients and terrestrial aridity (Pound et al., 2012).

While qualitative warmth during the MCO and cooling during the MMCT are well supported by geologic evidence, the quantitative evolution of global surface temperatures during these periods remains unclear. Benthic foraminiferal oxygen isotope records (benthic $\delta^{18}O$) have provided high-resolution information on global climate throughout the early and middle Miocene (Holbourn et al., 2014, 2015), but surface temperature proxy records at similar resolution are lacking. As a result of this gap, estimates of middle Miocene global warmth range anywhere from ~5 °C (Westerhold et al., 2020) to more than 10 °C above modern (Burls et al., 2021; Herbert et al., 2022).

Existing Northern Hemisphere sea surface temperature (SST) records are limited to sites in the eastern North Atlantic and North Sea (Herbert et al., 2016, 2020; Super et al., 2020; Sangiorgi et al., 2021; Fig. 1). These sites are influenced by regional dynamics of the North Atlantic Current, so SSTs at these sites may not be representative of broader Miocene Northern Hemisphere temperatures. In addition, the temporal resolution of these records does not resolve orbital-scale SST variability. Higher-resolution records from other regions are needed to constrain the Miocene evolution of Northern Hemisphere SSTs.

Here, we present high-resolution SST proxy data from the North Pacific spanning the entire MCO and MMCT. We measure the unsaturation ratios of alkenones ($U^{k'}_{37}$ [see Supplemental Material[1]]) from Ocean Drilling Program (ODP) Site 884 in the northwest Pacific (Rea et al., 1993; see the Supplemental Material[1] for site description). $U^{k'}_{37}$ SST reconstructions are largely robust to species effects (Villanueva et al., 2002), assumptions of past seawater chemistry, and methods of calibration to SST (Müller et al., 1998; Tierney and Tingley, 2018), and this proxy has been successfully applied to quantifying global mean annual SSTs in the late Miocene (Herbert et al., 2016). High core recovery (>90%) and magnetic reversal stratigraphy (Table S1 in the Supplemental Material) provide a continuous and well-dated section for high-resolution records of the MCO and MMCT at Site 884 (see the Supplemental Material for age model). Our record extends continuous records of SSTs in the North Pacific to span the past 18 million years.

RESULTS AND DISCUSSION

Our measurements of $U^{k'}_{37}$ at Site 884 provide a continuous high-resolution (6 k.y. average sampling interval) record of SSTs in the subpolar North Pacific from 18.2 to 12.6 Ma, with lower resolution (54 k.y.) data to 8.8 Ma. After column chromatography, alkenones were analyzed using gas chromatographic or high-performance liquid chromatographic methods (see the Supplemental Material for analytical methods). $U^{k'}_{37}$ varied between 0.393 and 0.882, providing reconstructed SSTs between 10.6 and 25.4 °C. We apply the calibration of Müller et al. (1998), though other choices of calibration do not significantly affect the reconstructed SSTs for the range of $U^{k'}_{37}$ obtained (Tierney and Tingley, 2018).

Previous work suggests seasonal biases in the modern application of the $U^{k'}_{37}$ proxy in the subpolar North Pacific, although the implications for

Jared E. Nirenberg https://orcid.org/0000-0002-5830-298X
*jared_nirenberg@brown.edu

[1]Supplemental Material. Alkenone analytical methods, site description, and age model for ODP Site 884, calculation of SST anomalies, Figures S1–S6, and Tables S1–S2. Please visit https://doi.org/10.1130/GEOL.S.27306198 to access the supplemental material; contact editing@geosociety.org with any questions.

CITATION: Nirenberg, J.E., and Herbert, T.D., 2024, North Pacific warmth synchronous with the Miocene Climatic Optimum: Geology, v. XX, p. , https://doi.org/10.1130/G52432.1

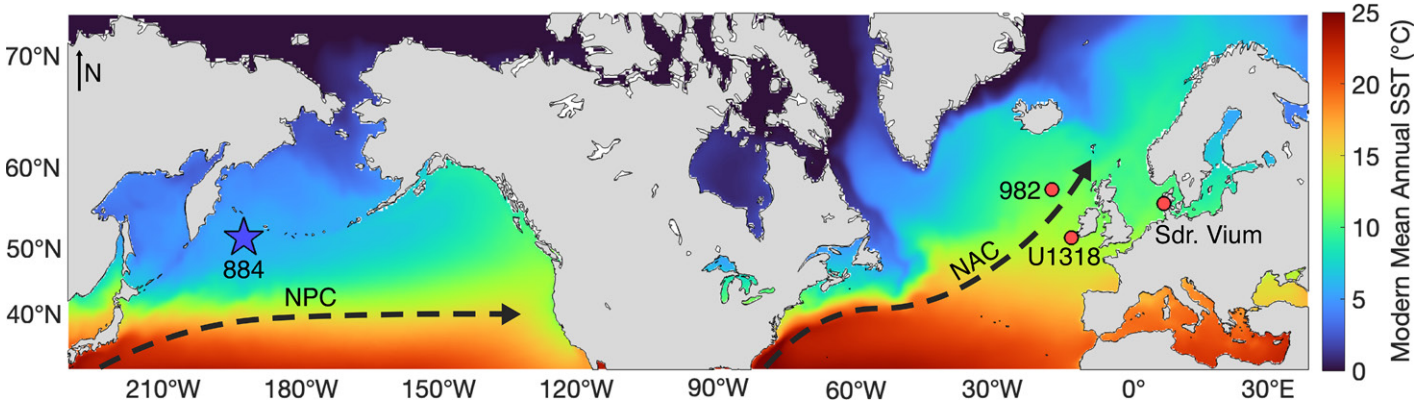

Figure 1. Site locations of northern subpolar $U^{k'}_{37}$ records during the early–middle Miocene. Data from Ocean Drilling Program (ODP) Site 884 (blue star) were generated in this study and from Herbert et al. (2016). Data from ODP Site 982, Integrated Ocean Drilling Program (IODP) Site U1318, and borehole Sdr. Vium (red circles) are from Herbert et al. (2016, 2020), Sangiorgi et al. (2021), and Super et al. (2020). Generalized paths of North Atlantic Current (NAC) and North Pacific Current (NPC) are shown as dashed arrows. SST—sea surface temperature.

Miocene interpretations are uncertain. The majority of alkenone production in the region occurs between July and November (Harada et al., 2006), which average 2.9 °C warmer than mean annual SSTs at Site 884 (Huang et al., 2021). Regional core-top $U^{k'}_{37}$ correlates most strongly with June through August monthly SSTs (Tierney and Tingley, 2018), which are 2.3 °C warmer than mean annual SSTs at Site 884 (Huang et al., 2021). While winter light limitation was similar, differences in the seasonal variation of SSTs and nutrient availability between the Miocene and modern are unknown, complicating any assumption of similar biases in $U^{k'}_{37}$ as well.

In addition, alkenone concentrations were strongly anti-correlated with $U^{k'}_{37}$, with warmer proxy values corresponding to exponentially lower alkenone concentrations (Fig. S1 in the Supplemental Material). Our Miocene anti-correlation implies higher production of alkenones associated with cooler temperatures at Site 884, potentially biasing reconstructed SSTs toward colder values. Because of conflicting directions for potential biases, we interpret $U^{k'}_{37}$ at Site 884 as representative of mean annual SSTs during the Miocene, though we acknowledge the potential for some bias (<3 °C) toward warmer seasonal temperatures.

Early–Middle Miocene Temperature Evolution in the North Pacific

We find a pronounced SST maximum in the North Pacific synchronous within age uncertainties to the MCO as defined by benthic $\delta^{18}O$ records (Holbourn et al., 2014, 2015). Long-term mean temperatures during the MCO peak above 22 °C, more than 16 °C warmer than the modern mean annual SST at Site 884. Though changes in SSTs at high latitudes were likely amplified compared to the global mean (Liu et al., 2022), these temperatures are more consistent with high-end estimates of MCO global warmth of at least 10 °C warmer than modern (Herbert et al., 2022: ~12 °C; Burls et al., 2021: ~11.5 °C) than more modest estimates (Westerhold et al., 2020: ~5 °C).

The coincident timing of Miocene warmth and subsequent cooling in the North Pacific with analogous changes in benthic $\delta^{18}O$ establishes a globally synchronous evolution of Miocene ocean temperatures. The benthic $\delta^{18}O$ signal originates from the southern high latitudes, which were the source of both bottom water formation and terrestrial ice volume during the early–middle Miocene (Shevenell et al., 2008), controlling both deep sea temperatures and seawater $\delta^{18}O$. Geologic records from Antarctica and the polar Southern Ocean (Lewis et al., 2008; Warny et al., 2009; Pierce et al., 2017) corroborate reduced MCO ice volume and ice sheet expansion during the MMCT interpreted from benthic $\delta^{18}O$ (Holbourn et al., 2014, 2015). While previous temperature records have found high-latitude cooling events during the MMCT, either preceding or coincident with the Mi3 glaciation between 13.8 and 14.2 Ma (Shevenell et al., 2004; Super et al., 2020; Sangiorgi et al., 2021), ours captures the significant warming at the onset of the MCO as well as MMCT cooling in a continuous record at a single site.

In light of ice-distal SST records from both the North Atlantic and North Pacific, the Miocene decay and subsequent growth of ice sheets in Antarctica cannot be attributed primarily to regional dynamics (Shevenell et al., 2008; Hou et al., 2023) but rather as part of global temperature changes. Direct ice sheet feedbacks (ice albedo, positions of Southern Hemisphere frontal zones, etc.) from the Antarctic would have been insufficient to explain high-latitude warmth in both the North Pacific and North Atlantic. Changes in greenhouse gas concentrations likely provided this global forcing, though direct evidence for synchronous changes in atmospheric pCO_2 proxy records have yielded widely varying results (Cenozoic CO_2 Proxy Integration Project [CENCO$_2$PIP] Consortium, 2023, and references therein; Fig. 2A). While pCO_2 proxies show a local maximum coinciding with the MCO, the increase in atmospheric pCO_2 appears to lag the increase in SSTs at Site 884 and in benthic $\delta^{18}O$ (Fig. 2). However, we caution this may be an artifact of low pCO_2 proxy data density covering the Early Miocene before the MCO. The eruption of the Columbia River Flood Basalts (northwestern United States) is commonly considered the source of this inorganic carbon to the ocean-atmosphere system (Holbourn et al., 2015; Sosdian et al., 2020), but this mechanism is challenged by the later timing of eruptions with respect to warming (Kasbohm and Schoene, 2018) and questions regarding the ability for these emissions to cause such long-sustained (~3 m.y.) warmth. While flood volcanism may have contributed to peak warmth early during the MCO, elevated tectonic degassing (Herbert et al., 2022) provides a more sustained mechanism of greenhouse gas emissions on million-year time scales. The beginning of long-term cooling after 15 Ma aligns with declining seafloor spreading rates (Fig. S2). Slowing mantle degassing could explain the initiation of cooling, culminating in passing a glaciation threshold (DeConto et al., 2008) during the Mi3 glaciation. However, our temperature records alone cannot distinguish between the importance of reductions in CO_2 sources to the atmosphere and increasing weathering sinks, such as the uplift of highly weatherable silicates in the tropics (Park et al., 2020). Changes in carbon cycling within the ocean-atmosphere system (Holbourn et al., 2015) were associated with climate variability on shorter time scales (tens to hundreds of thousands of years) imposed on these longer-term (millions of years) tectonic forcings.

High-Resolution Records Reveal Rapid Transitions and Orbital-Scale Variability

Our high-resolution data reveal rapid warming at the beginning of the MCO as well as cooling synchronous with East Antarctic Ice Sheet

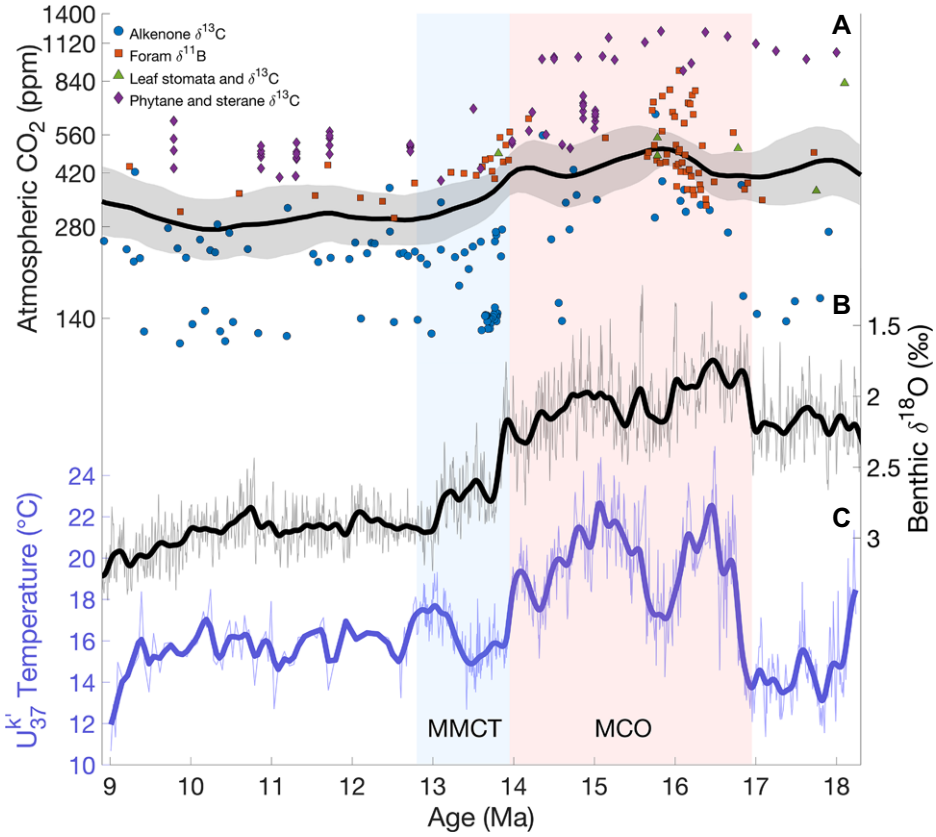

Figure 2. (A) pCO_2 proxy estimates and 100 k.y. smoothed average (black line; gray shading represents 95% confidence interval) from Cenozoic CO_2 Proxy Integration Project ($CENCO_2PIP$) Consortium (2023) along with phytane and sterane data from Witkowski et al. (2024). (B) Benthic $\delta^{18}O$ from Westerhold et al. (2020). (C) Alkenone-derived sea surface temperatures produced in this work from Ocean Drilling Program (ODP) Site 884. In B and C, individual data (thin line) are shown along with Gaussian-weighted smoothed average (thick line). MMCT—Middle Miocene Climate Transition; MCO—Miocene Climatic Optimum.

expansion during the MMCT. SSTs at Site 884 warm more than 7°C within 50 k.y. after 17 Ma (Fig. 3), a time scale shorter than that over which tectonic processes could have been the forcing mechanism. Although our reported timing of this warming is younger than that observed in the benthic $\delta^{18}O$ records (Holbourn et al., 2015), we interpret these as synchronous within error of our age model (Supplemental Material). In addition, SSTs in the North Pacific cool 4 °C after 14 Ma, though a gap in sediment recovery between cores prevents precise determination of the duration of cooling. This cooling event aligns with the abrupt expansion of the East Antarctic Ice Sheet observed in Antarctic geologic records (Lewis et al., 2008; Pierce et al., 2017) and in benthic $\delta^{18}O$ records (Shevenell et al., 2004; Holbourn et al., 2014) as well as decreasing atmospheric pCO_2 observed in some proxy records (Badger et al., 2013; Raitzsch et al., 2021; Witkowski et al., 2024).

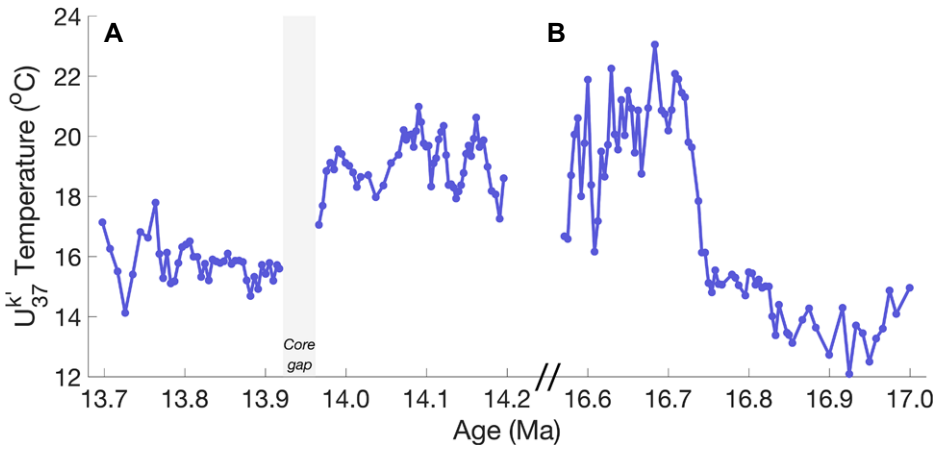

Figure 3. High-resolution alkenone-derived sea surface temperatures (SSTs) from Ocean Drilling Program (ODP) Site 884 during two key climatic transitions. (A) Mi3 glaciation during Middle Miocene Climate Transition, where SSTs cool ~4 °C after 14 Ma. (B) Onset of Miocene Climatic Optimum, when SSTs abruptly warm ~7 °C after 17 Ma. Discrepancies between timing of these transitions and those in benthic $\delta^{18}O$ are within error of age model for Site 884.

North Pacific SSTs during the MCO were highly variable, with glacial-interglacial cycles of as much as 6 °C in amplitude (Fig. 3) and a longer cooler interval surrounding the Mi2 glaciation (Miller et al., 1991) after 16 Ma (Fig. 2). Significant periodicities correspond to orbital frequencies near eccentricity (109 k.y., 99% confidence level) and obliquity (43 k.y., 90% confidence level) across the high-resolution record (Fig. S3). The large amplitude of orbital-scale temperature variability, particularly during the MCO, is consistent with large variability found in contemporaneous $\delta^{18}O$ (Holbourn et al., 2014, 2015), atmospheric pCO_2 proxies (Greenop et al., 2014), and Antarctic ice sheet extent (Levy et al., 2016) on orbital time scales. Our record confirms that temperature variability in the high latitudes distant from Southern Hemisphere ice sheets accompanied these changes as well.

Enhanced North Atlantic Current during Miocene Global Warmth

To assess the context of North Pacific temperatures within the northern subpolar regions, we compile Miocene $U^{k'}_{37}$ records from sites between 50°N and 60°N (Herbert et al., 2016, 2020; Super et al., 2020; Sangiorgi et al., 2021; Fig. 4; Fig S4). SST anomalies in the North Atlantic relative to modern mean annual SST were persistently higher than in the North Pacific throughout the Miocene, resulting in a larger than modern gradient between the basins. While the gradient appears to reduce during the MCO, we caution that this may be an artifact of proxy saturation ($U^{k'}_{37}$ approaches 1) at North Atlantic sites. The proxy response to further SST variability at these high temperatures is likely truncated, whereas North Pacific $U^{k'}_{37}$ is much further from saturation. Because reconstructed SSTs in the North Atlantic depend more on the choice of linear (Müller et al., 1998) or nonlinear (Tierney and Tingley, 2018) calibrations, our reconstructed inter-basin gradient has higher uncertainty during the MCO.

The gradient between North Pacific and North Atlantic SST anomalies (Fig. 4) suggests persistent differences in poleward oceanic heat transport between the two basins. While the modern North Atlantic is warmer than

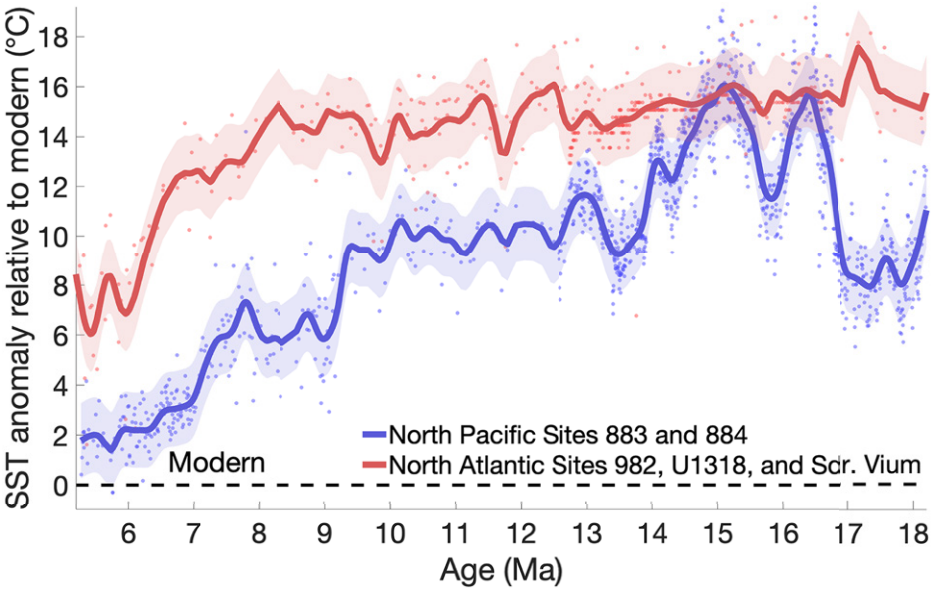

Figure 4. Miocene sea surface temperature (SST) anomalies relative to modern mean annual SSTs for high-latitude Northern Hemisphere sites. Data from Ocean Drilling Program (ODP) Sites 883 and 884 are from this study and Herbert et al. (2016). Data from ODP Site 982, Integrated Ocean Drilling Program (IODP) Site U1318, and borehole Sdr. Vium are from Herbert et al. (2016, 2020), Sangiorgi et al. (2021), and Super et al. (2020). Individual data are shown as points with a Gaussian-weighted smoothed average (thick line; shading represents one standard error range of calibration of Müller et al., 1998).

the North Pacific due to the greater poleward influence of the North Atlantic Current (NAC) compared to the North Pacific Current (Fig. 1), these differences were enhanced throughout the Miocene (Fig. S5). Super et al. (2020) hypothesized an invigorated NAC as responsible for extreme North Atlantic warmth, extending into the mid-latitudes as well, and our North Pacific record confirms this warmth was exaggerated in the Atlantic basin. These proxy records contradict predictions from model simulations (Burls et al., 2021) of a reduced or even reversed Miocene temperature gradient between the northern ocean basins (Fig. S6). A stronger inter-basin gradient during the Miocene, when the Central American Seaway was open, also challenges the idea of a weaker NAC prior to seaway closure during the Pliocene (Haug and Tiedemann, 1998). While these paleotemperature records alone cannot directly rule out effects of other possible mechanisms, such as cloud radiative feedbacks and atmospheric heat transport, greater northward oceanic heat transport in the Atlantic basin provides a compelling potential mechanism for enhanced Miocene warmth observed in the North Atlantic.

CONCLUSIONS

Our high-resolution SST proxy record spanning the entire MCO and MMCT at a single site extends our understanding of continuous temperature evolution in the North Pacific over the past 18 million years. Elevated temperatures in the northern high-latitudes coincide with minimal Antarctic ice sheet volumes and higher bottom water temperatures, showing that the MCO was a globally synchronous climate interval in the high latitudes. The bipolar nature of warmth between ca. 17 and 14 Ma suggests a global forcing mechanism, likely elevated greenhouse gas concentrations, though proxy constraints on these concentrations vary widely (Cenozoic CO_2 Proxy Integration Project [$CENCO_2PIP$] Consortium, 2023). The coincidence of high SST variability on orbital time scales in the North Pacific with similarly large variations in benthic $\delta^{18}O$ implies either large changes in atmospheric pCO_2 on these time scales or high sensitivity of Miocene climate to smaller changes in greenhouse gas concentrations or orbital forcing. While high-resolution temperature records from more regions are needed to assess the global pattern and magnitude of temperature variability, the synchronous timing of early–middle Miocene warmth in both the North Pacific and Antarctic provides strong circumstantial evidence for a common forcing.

ACKNOWLEDGMENTS

This study used samples and data provided by the International Ocean Discovery Program (IODP) and its predecessors. Funding was provided by National Science Foundation grants 1635127 and 2202760 to Herbert. We thank Jonah Bernstein-Schalet, Emily Clements, and Sofía Gilroy for their assistance in sample preparation. Thanks also to Junsheng Nie and two anonymous reviewers for their constructive reviews. Alkenone data is also available at https://doi.pangaea.de/10.1594/PANGAEA.965068.

REFERENCES CITED

Badger, M.P.S., Lear, C.H., Pancost, R.D., Foster, G.L., Bailey, T.R., Leng, M.J., and Abels, H.A., 2013, CO_2 drawdown following the middle Miocene expansion of the Antarctic Ice Sheet: Paleoceanography, v. 28, p. 42–53, https://doi.org/10.1002/palo.20015.

Burls, N.J., et al., 2021, Simulating Miocene warmth: Insights from an opportunistic multi-model ensemble (MioMIP1): Paleoceanography and Paleoclimatology, v. 36, https://doi.org/10.1029/2020PA004054.

Cenozoic CO_2 Proxy Integration Project ($CENCO_2PIP$) Consortium, 2023, Toward a Cenozoic history of atmospheric CO_2: Science, v. 382, https://doi.org/10.1126/science.adi5177.

DeConto, R.M., Pollard, D., Wilson, P.A., Pälike, H., Lear, C.H., and Pagani, M., 2008, Thresholds for Cenozoic bipolar glaciation: Nature, v. 455, p. 652–656, https://doi.org/10.1038/nature07337.

Greenop, R., Foster, G.L., Wilson, P.A., and Lear, C.H., 2014, Middle Miocene climate instability associated with high-amplitude CO_2 variability: Paleoceanography, v. 29, p. 845–853, https://doi.org/10.1002/2014PA002653.

Harada, N., Sato, M., Shiraishi, A., and Honda, M.C., 2006, Characteristics of alkenone distributions in suspended and sinking particles in the northwestern North Pacific: Geochimica et Cosmochimica Acta, v. 70, p. 2045–2062, https://doi.org/10.1016/j.gca.2006.01.024.

Haug, G.H., and Tiedemann, R., 1998, Effect of the formation of the Isthmus of Panama on Atlantic Ocean thermohaline circulation: Nature, v. 393, p. 673–676, https://doi.org/10.1038/31447.

Herbert, T.D., Lawrence, K.T., Tzanova, A., Peterson, L.C., Caballero-Gill, R., and Kelly, C.S., 2016, Late Miocene global cooling and the rise of modern ecosystems: Nature Geoscience, v. 9, p. 843–847, https://doi.org/10.1038/ngeo2813.

Herbert, T.D., Rose, R., Dybkjær, K., Rasmussen, E.S., and Śliwińska, K.K., 2020, Bihemispheric warming in the Miocene Climatic Optimum as seen from the Danish North Sea: Paleoceanography and Paleoclimatology, v. 35, https://doi.org/10.1029/2020PA003935.

Herbert, T.D., Dalton, C.A., Liu, Z., Salazar, A., Si, W., and Wilson, D.S., 2022, Tectonic degassing drove global temperature trends since 20 Ma: Science, v. 377, p. 116–119, https://doi.org/10.1126/science.abl4353.

Holbourn, A., Kuhnt, W., Lyle, M., Schneider, L., Romero, O., and Andersen, N., 2014, Middle Miocene climate cooling linked to intensification of eastern equatorial Pacific upwelling: Geology, v. 42, p. 19–22, https://doi.org/10.1130/G34890.1.

Holbourn, A., Kuhnt, W., Kochhann, K.G.D., Andersen, N., and Sebastian Meier, K.J., 2015, Global perturbation of the carbon cycle at the onset of the Miocene Climatic Optimum: Geology, v. 43, p. 123–126, https://doi.org/10.1130/G36317.1.

Hou, S., Stap, L.B., Paul, R., Nelissen, M., Hoem, F.S., Ziegler, M., Sluijs, A., Sangiorgi, F., and Bijl, P.K., 2023, Reconciling Southern Ocean fronts equatorward migration with minor Antarctic ice volume change during Miocene cooling: Nature Communications, v. 14, 7230, https://doi.org/10.1038/s41467-023-43106-4.

Huang, B., Liu, C., Banzon, V., Freeman, E., Graham, G., Hankins, B., Smith, T., and Zhang, H.-M., 2021, Improvements of the Daily Optimum Interpolation Sea Surface Temperature (DOISST) version 2.1: Journal of Climate, v. 34, p. 2923–2939, https://doi.org/10.1175/JCLI-D-20-0166.1.

Kasbohm, J., and Schoene, B., 2018, Rapid eruption of the Columbia River flood basalt and correlation with the mid-Miocene climate optimum: Science Advances, v. 4, https://doi.org/10.1126/sciadv.aat8223.

Levy, R., et al., 2016, Antarctic ice sheet sensitivity to atmospheric CO_2 variations in the early to mid-Miocene: Proceedings of the National Academy of Sciences of the United States of America, v. 113, p. 3453–3458, https://doi.org/10.1073/pnas.1516030113.

Lewis, A.R., et al., 2008, Mid-Miocene cooling and the extinction of tundra in continental Antarctica: Proceedings of the National Academy of Sciences of the United States of America, v. 105, p. 10,676–10,680, https://doi.org/10.1073/pnas.0802501105.

Liu, X., Huber, M., Foster, G.L., Dessler, A., and Zhang, Y.G., 2022, Persistent high latitude amplification of the Pacific Ocean over the past 10 million years: Nature Communications, v. 13, 7310, https://doi.org/10.1038/s41467-022-35011-z.

Miller, K.G., Wright, J.D., and Fairbanks, R.G., 1991, Unlocking the Ice House: Oligocene-Miocene oxygen isotopes, eustasy, and margin erosion: Journal of Geophysical Research, v. 96, p. 6829–6848, https://doi.org/10.1029/90JB02015.

Müller, P.J., Kirst, G., Ruhland, G., von Storch, I., and Rosell-Melé, A., 1998, Calibration of the alkenone paleotemperature index $U_{37}^{K'}$ based on core-tops from the eastern South Atlantic and the global ocean (60°N-60°S): Geochimica et Cosmochimica Acta, v. 62, p. 1757–1772, https://doi.org/10.1016/S0016-7037(98)00097-0.

Park, Y., Maffre, P., Goddéris, Y., Macdonald, F.A., Anttila, E.S.C., and Swanson-Hysell, N.L., 2020, Emergence of the Southeast Asian islands as a driver for Neogene cooling: Proceedings of the National Academy of Sciences of the United States of America, v. 117, p. 25,319–25,326, https://doi.org/10.1073/pnas.2011033117.

Pierce, E.L., van de Flierdt, T., Williams, T., Hemming, S.R., Cook, C.P., and Passchier, S., 2017, Evidence for a dynamic East Antarctic ice sheet during the mid-Miocene climate transition: Earth and Planetary Science Letters, v. 478, p. 1–13, https://doi.org/10.1016/j.epsl.2017.08.011.

Pound, M.J., Haywood, A.M., Salzmann, U., and Riding, J.B., 2012, Global vegetation dynamics and latitudinal temperature gradients during the Mid to Late Miocene (15.97–5.33 Ma): Earth-Science Reviews, v. 112, p. 1–22, https://doi.org/10.1016/j.earscirev.2012.02.005.

Raitzsch, M., Bijma, J., Bickert, T., Schulz, M., Holbourn, A., and Kučera, M., 2021, Atmospheric carbon dioxide variations across the middle Miocene climate transition: Climate of the Past, v. 17, p. 703–719, https://doi.org/10.5194/cp-17-703-2021.

Rea, D.K., Basov, I.A., Janecek, T.R., Palmer-Julson, A., et al., eds., 1993, Proceedings of the Ocean Drilling Program, Initial Reports, Volume 145: College Station, Texas, Ocean Drilling Program, https://doi.org/10.2973/odp.proc.ir.145.1993.

Sangiorgi, F., Quaijtaal, W., Donders, T.H., Schouten, S., and Louwye, S., 2021, Middle Miocene temperature and productivity evolution at a northeast Atlantic shelf site (IODP U1318, Porcupine Basin): Global and regional changes: Paleoceanography and Paleoclimatology, v. 36, https://doi.org/10.1029/2020PA004059.

Shevenell, A.E., Kennett, J.P., and Lea, D.W., 2004, Middle Miocene Southern Ocean cooling and Antarctic cryosphere expansion: Science, v. 305, p. 1766–1770, https://doi.org/10.1126/science.1100061.

Shevenell, A.E., Kennett, J.P., and Lea, D.W., 2008, Middle Miocene ice sheet dynamics, deep-sea temperatures, and carbon cycling: A Southern Ocean perspective: Geochemistry, Geophysics, Geosystems, v. 9, Q02006, https://doi.org/10.1029/2007GC001736.

Sosdian, S.M., Babila, T.L., Greenop, R., Foster, G.L., and Lear, C.H., 2020, Ocean Carbon Storage across the middle Miocene: A new interpretation for the Monterey Event: Nature Communications, v. 11, 134, https://doi.org/10.1038/s41467-019-13792-0.

Super, J.R., Thomas, E., Pagani, M., Huber, M., O'Brien, C.L., and Hull, P.M., 2020, Miocene evolution of North Atlantic sea surface temperature: Paleoceanography and Paleoclimatology, v. 35, https://doi.org/10.1029/2019PA003748.

Tierney, J.E., and Tingley, M.P., 2018, BAYSPLINE: A new calibration for the alkenone paleothermometer: Paleoceanography and Paleoclimatology, v. 33, p. 281–301, https://doi.org/10.1002/2017PA003201.

Villanueva, J., Flores, J.A., and Grimalt, J.O., 2002, A detailed comparison of the $U^{k'}_{37}$ and coccolith records over the past 290 kyears: Implications to the alkenone paleotemperature method: Organic Geochemistry, v. 33, p. 897–905, https://doi.org/10.1016/S0146-6380(02)00067-0.

Warny, S., Askin, R.A., Hannah, M.J., Mohr, B.A.R., Raine, J.I., Harwood, D.M., Florindo, F., and the SMS Science Team, 2009, Palynomorphs from a sediment core reveal a sudden remarkably warm Antarctica during the middle Miocene: Geology, v. 37, p. 955–958, https://doi.org/10.1130/G30139A.1.

Westerhold, T., et al., 2020, An astronomically dated record of Earth's climate and its predictability over the last 66 million years: Science, v. 369, p. 1383–1387, https://doi.org/10.1126/science.aba6853.

Witkowski, C.R., von der Heydt, A.S., Valdes, P.J., van der Meer, M.T.J., Schouten, S., and Sinninghe Damsté, J.S., 2024, Continuous sterane and phytane $\delta^{13}C$ record reveals a substantial pCO_2 decline since the mid-Miocene: Nature Communications, v. 15, 5192, https://doi.org/10.1038/s41467-024-47676-9.

Printed in the USA